Infrared Spectroscopy of Size-Selected Benzene−Water Cluster Cations $[C_6H_6-(H_2O)_n]^+$ ($n = 1-23$): Hydrogen Bond Network Evolution and Microscopic Hydrophobicity

Mitsuhiko Miyazaki,† Asuka Fujii,* Takayuki Ebata,‡ and Naohiko Mikami*

Department of Chemistry, Graduate School of Science, Tohoku University, Sendai 980-8578, Japan

Received: September 15, 2004

Infrared (IR) spectra of size-selected benzene−water cluster cations ($[C_6H_6-(H_2O)_n]^+$, $n = 1-23$) were measured in the OH and CH stretch regions to investigate the cluster structures, especially at large sizes. In the size range of $n = 4-23$, the IR spectra show features almost identical to those of protonated water cluster cations $H^+(H_2O)_n$, consistent with the occurrence of the intracluster proton-transfer reaction from the benzene moiety to the water moiety, as suggested in the previous IR and electronic spectroscopic studies of the small-sized clusters. The structure of the protonated water moiety was found to be almost the same as that of $H^+(H_2O)_n$ up to $n = 23$, including the characteristic three-dimensional cage structure at $n = 21$. On the basis of the IR spectra, it was demonstrated that the phenyl radical participates in the direct solvation of the H_3O^+ core in the clusters of $n \lesssim 10$. In the larger sized clusters, while the protonated water moiety forms the exclusive hydrogen bond network, the phenyl radical is finally pushed out to the exterior of the network, reflecting the microscopic hydrophobicity of the aromatic ring.

Introduction

The proton is the simplest and most important cation in nature, and its interaction with water, which is the most abundant solvent on the earth, has been subject to much interest from various fields of science.[1−4] To establish a microscopic picture of the solvation of the proton, a great number of studies have been carried out for the protonated water cluster $H^+(H_2O)_n$ in the gas phase.[4−30] Detailed energetics of the proton hydration has been determined by mass spectrometric methods,[4−10] and many computational studies on the geometric structures, energetics, and dynamical behavior of the protonated water clusters have been carried out.[11−21] However, experimental information on the structures of $H^+(H_2O)_n$ is still very limited, especially for large-sized clusters of $n \geq 10$. Structures of small-sized $H^+(H_2O)_n$ of $n \leq 8$ have been extensively studied by infrared (IR) spectroscopy and density functional theory (DFT) calculations.[22−25] It has been shown that the small-sized clusters have chain-type structures, in which hydrogen-bonded linear water chains develop from the hydronium ion (H_3O^+ or $H_5O_2^+$) site located at the center of the clusters.[22−25] Two-dimensional (2-D) net-type structures can be formed by the binding of the terminal site within a water chain, and a preliminary step of such a process is found in $n = 7-8$.[24] However, structures of larger sized clusters, which would be a key to understanding the bulk system, have not been experimentally probed for a long time. The only exception is the $H^+(H_2O)_{21}$ cluster, which is a well-known magic number in the mass spectra of $H^+(H_2O)_n$ produced by any ionization method.[4,8,9,26,27] The extraordinary stability of the $n = 21$ cluster has been interpreted in terms of the regular dodecahedral cage structure encaging a water molecule within the cavity, and mass spectrometric studies have indicated the presence of 10 dangling OH bonds in the cluster.[28] Very recently, IR spectra of $H^+(H_2O)_n$ of $n \leq 27$ were simultaneously reported by our group and Shin et al.[29,30] It was demonstrated that the hydrogen bond network of $H^+(H_2O)_n$ develops into 2-D net-type structures at $n \approx 10$, and the 3-D closed-cage structure formation is completed at $n = 21$, consistent with the previous mass spectrometric and theoretical calculation studies for $n = 21$. In addition, it was found that the clusters of $n > 21$ also hold the 3-D cage structures.

To examine the microscopic view of the hydrated proton, not only the protonated water clusters but also clusters involving molecules other than water are important because impurity molecules generally exist in actual aqueous solutions. Moreover, such a cluster can be a model of various solutions containing some solutes. However, the effects of the impurity molecules on the hydrogen bond structures have not yet been fully understood. As for small-sized protonated water clusters, IR spectroscopic studies on $X-H^+(H_2O)_n$, $n \leq 6$ ($X = CH_3OH$ [ref 31], $(CH_3)_2O$ [ref 32], and phenoxy radical ($C_6H_5O^\bullet$) [refs 33 and 34]), showed that these systems have structures nearly identical to those of pure $H^+(H_2O)_{n+1}$ replacing a water molecule with X. For larger sized cluster cations, many mass spectrometric studies have been carried out to probe their structures. For example, it has been reported that $H^+(CH_3OH)_m(H_2O)_n$ shows magic numbers at $m + n = 21$, suggesting the compatibility between water and methanol to form a dodecahedral cage.[35] In hydrated alkali-metal cluster cations, which can be potential analogues to protonated water, it is known that K^+, Rb^+, and Cs^+ show the magic number at $n = 20$ and cage structures similar to that of a protonated water cluster are supposed, while Li^+ and Na^+ show no clear magic number.[4,36−40] Such different behavior of hydrated alkali-metal clusters is considered a result of a balance in energy between hydration and hydrogen bonding.[40] Although structures of some specific sizes, such as $n = 20$ or 21, of clusters are easily inferred on the basis of mass spectrometry, actual structural similarity between hydrated cluster cations and $H^+(H_2O)_n$ has not yet been confirmed.

* To whom correspondence should be addressed. E-mail: asuka@qclhp.chem.tohoku.ac.jp (A.F.) nmikami@qclhp.chem.tohoku.ac.jp (N.M.). Fax: 81-022-217-6785.

† Present address: Department of Chemistry, Graduate School of Science, Kyoto University, Kyoto 606-8502, Japan.

‡ Present address: Department of Chemistry, Graduate School of Science, Hiroshima University, Higashihiroshima 739-8526, Japan.

10.1021/jp045823f CCC: $27.50
Published on Web 11/04/2004

In this paper, we report an IR spectroscopic study of benzene−water cluster cations $[C_6H_6-(H_2O)_n]^+$, $n = 1-23$, as a model system of $H^+(H_2O)_n$ including an aromatic impurity to reveal its effects on water hydrogen bond network structures. Previous IR and electronic spectroscopic studies have demonstrated that the $[C_6H_6-(H_2O)_n]^+$ cluster cation exhibits the intracluster proton-transfer reaction from a C−H bond of $C_6H_6^+$ to the water moiety, and the clusters can be regarded as $[C_6H_5^{\bullet}-H^+(H_2O)_n]$ with $n \geq 4$.[41−43] Mass spectrometry of photoionized $[C_6H_6-(H_2O)_n]^+$ clusters with $n \approx 20$ showed a size distribution similar to those of $H^+(H_2O)_n$, and the magic number at $n = 21$ was also found.[44] This result has also been understood by the proton-transfer reaction from $C_6H_6^+$. Therefore, the $[C_6H_6-(H_2O)_n]^+$ ($n \geq 4$) clusters are regarded to be protonated water with phenyl radical as an impurity, and are expected to be an appropriate system to study the effects of the aromatic impurity on the hydrogen bond network.

Experiment

IR spectra of the $[C_6H_6-(H_2O)_n]^+$ cluster cations were recorded by using a mass spectrometer equipped with linearly aligned tandem quadrupole mass filters connected by an octopole ion guide. The details of the apparatus have already been described in previous papers,[41,42] and here we give only a brief description. The $[C_6H_6-(H_2O)_n]^+$ cluster cations were produced with collisions between photoionized benzene and water molecules in a channel nozzle followed by an adiabatic expansion. Vapors of benzene and water were picked up by buffer Ne gas, and the gaseous mixture was expanded into a vacuum through the channel nozzle equipped at a pulsed valve. The total stagnation pressure of the gaseous mixture was typically 3 atm. Benzene was resonantly ionized via the S_1-S_0 6^1_0 transition within the channel nozzle by a second harmonic of a dye laser output, which was introduced into the channel through a side pinhole drilled at the vicinity of the pulsed valve. The produced $[C_6H_6-(H_2O)_n]^+$ cluster cations were size-selected by the first quadrupole mass filter and then were introduced into the octopole ion guide. Though the mass of $(C_6H_6)_4^+$ is the same as that of $[C_6H_6-(H_2O)_{13}]^+$ ($M = 312$ amu), the production of the former was totally suppressed by the control of the partial pressure of benzene. Within the octopole ion guide, the mass-selected cations were irradiated by a counterpropagating IR laser, and were sent to the second quadrupole mass filter, which was tuned to the mass of a fragment ion produced by the vibrational excitation. Thus, an IR spectrum of the size-selected cluster was recorded by measuring the fragment ion intensity while scanning the IR laser frequency. Although $[C_6H_6-(H_2O)_n]^+$ clusters larger than $n \approx 15$ produced several fragment species upon the vibrational excitation, we recorded the IR spectra by monitoring only the $n-1$ fragment ion channel, i.e., evaporation of one water molecule.

Results and Discussion

Figure 1 shows IR spectra of $[C_6H_6-(H_2O)_n]^+$ ($n = 1-23$) in the OH and CH stretch regions measured by monitoring the $n-1$ fragment ions. Relatively sharp bands appearing around 3700 cm^{-1} are attributed to free OH stretching vibrations and broad features around 3000−3500 cm^{-1} to hydrogen-bonded OH stretching vibrations of the water moiety.[22−25,41,43] Bands seen at around 3100 cm^{-1} for $n = 1-3$ are assigned to CH stretching vibrations of the aromatic moiety, but these bands are buried in much stronger hydrogen-bonded OH stretch bands for $n \geq 4$.[41] The gap in the spectra in the region of 3460−3520 cm^{-1} is caused by undesired depletion of the IR light due to the water impurities in the nonlinear optical crystal used.

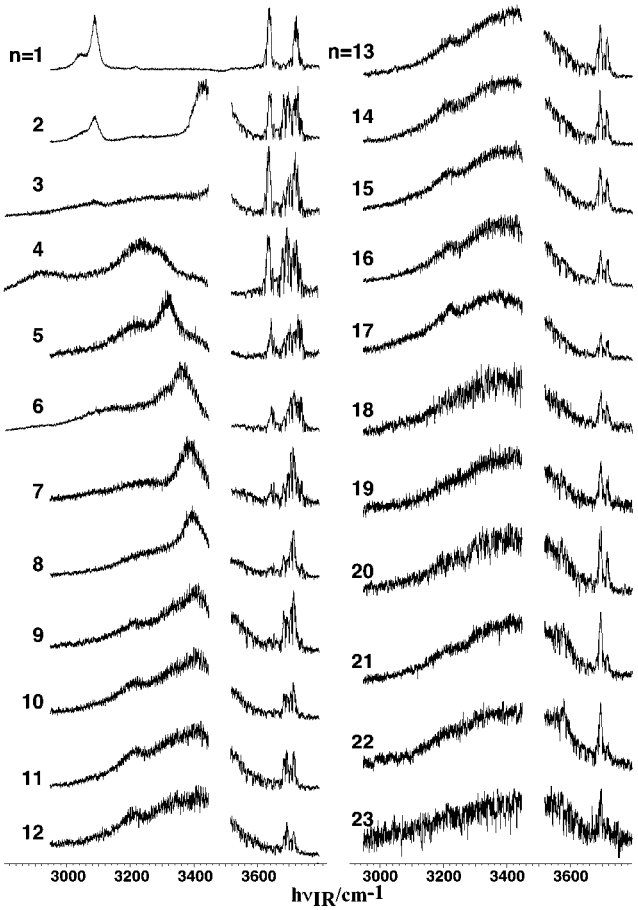

Figure 1. IR spectra of size-selected $[C_6H_6-(H_2O)_n]^+$ ($n = 1-23$) clusters in the OH and CH stretch regions. The spectral gaps seen around 3500 cm^{-1} are due to the IR absorption by the nonlinear crystal used to generate the IR light.

With an increase of the cluster size, the IR spectra show gradual changes in their features, reflecting the evolution of the hydrogen bond network. In our previous paper,[41] we reported the IR spectra of $[C_6H_6-(H_2O)_n]^+$ in the size range of $1 \leq n \leq 6$, and found that a very broad hydrogen-bonded OH band begins to appear at $n = 4$ and the CH stretching bands conversely disappear at this size. Moreover, the size-dependent spectral feature for $4 \leq n \leq 6$ was found to be very similar to those of $X-H^+(H_2O)_n$ ($X = H_2O$ [ref 24], CH_3OH [ref 31], and $(CH_3)_2O$ [ref 32]), which have the H_3O^+ (or $H_5O_2^+$) ion core at the center of the cluster. Therefore, we have concluded that the intracluster proton-transfer reaction from $C_6H_6^+$ to the water moiety occurs at $n \geq 4$ and the clusters can be regarded as $[C_6H_5^{\bullet}-H^+(H_2O)_n]$, as schematically shown in Figure 2a. The occurrence of the intracluster proton transfer has also been confirmed with electronic spectroscopy of the aromatic moiety.[42]

In accordance with our previous conclusion, the IR spectra for $n \geq 6$ also show features very similar to those of pure protonated water clusters, which have been reported very recently.[29,30] Figure 3 shows an example of the comparison between the IR spectra of $[C_6H_6-(H_2O)_n]^+$ and $[H_2O-H^+(H_2O)_n]$ in the size range of $n = 3-10$. Details of the IR spectroscopy of $[H_2O-H^+(H_2O)_n]$ were described in our previous paper.[29] It is clearly seen in Figure 3 that in the range of $n = 4-7$ both the clusters show very similar spectral features at the same size and the size dependence of the spectral feature is tentatively saturated at $n = 8-10$.

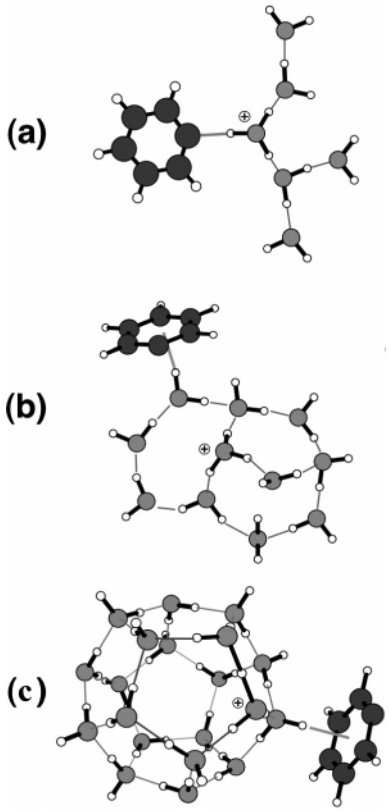

Figure 2. Schematic representations of structures of the $[C_6H_6-(H_2O)_n]^+$ cluster cations. (a) Chain-type hydrogen bond network for $n \leq 10$. The phenyl radical may solvate the H_3O^+ ion core directly. (b) Net-type hydrogen bond network for $10 \approx n \approx 20$. The phenyl radical locates at the exterior of the water moiety. (c) Cage-type hydrogen bond network for $n \geq 21$. The water cage formation is completed at $n = 21$, and the phenyl radical is attached on the water cage surface by the π hydrogen bond (see the text).

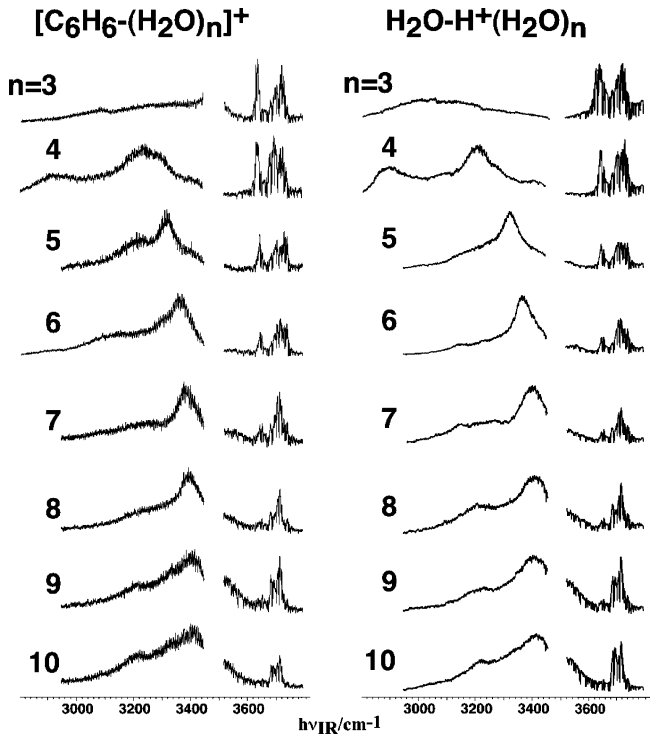

Figure 3. Comparison of the IR spectra of (left) $[C_6H_6-(H_2O)_n]^+$ and (right) $[H_2O-H^+(H_2O)_n]$ at $n = 3-10$. Note the correspondence of the cluster sizes (see the text).

Figure 4 is an expansion of the IR spectra of $[C_6H_6-(H_2O)_n]^+$ in the free OH stretch region. Four different types of bands are seen in this region. The pair of bands at 3650 and 3750 cm^{-1} is the symmetric (ν_1) and antisymmetric (ν_3) OH stretches of one-coordinated (single-acceptor) water, respectively, which locates at the terminal of a 1-D hydrogen bond chain. The free OH band at 3715 cm^{-1} is the dangling OH stretch of two-coordinated (single-acceptor−single-donor, AD) water in the hydrogen bond chain.[24,45,46] At $n \approx 10$, the ν_1 and ν_3 bands of the terminal water gradually disappear from the free OH stretching region while a new band alternately appears at ~3695 cm^{-1}. This new band is due to a dangling OH stretching vibration of three-coordinated (double-acceptor−single-donor, AAD) water,[45−49] which appears at a bridging site of hydrogen bond chains. At the same time, a small peak appears near 3200 cm^{-1} in the hydrogen-bonded OH stretching region. This band would be attributed to the hydrogen-bonded OH stretch of AAD water,[48−50] in accordance with the appearance of the dangling OH stretch band. The spectral change at $n \approx 10$ implies that, at this size region, a terminal water molecule of a hydrogen bond chain is bound to an AD water in another chain with a donation of one proton. Then, the terminal water is transformed to an AD water and the AD water to an AAD water. The disappearance of the ν_1 and ν_3 bands means that all the terminal waters are bound, so that the hydrogen bond structure becomes a 2-D net-type structure consisting of AD and AAD waters, as schematically shown in Figure 2b.

At $n \leq 10$, the intensity of the dangling OH stretch band of AD water is larger than that of AAD water, but the intensity ratio is reversed with an increase of the cluster size. Such a spectral change indicates a trend that an AD water molecule in a hydrogen bond chain is bound to another AD water molecule to be transformed to three-coordinated waters of double-donor−single-acceptor (ADD) and AAD types, respectively. A shoulder band appearing at ~3550 cm^{-1} from the $n \approx 18$ cluster also supports this transformation, since this band has been ascribed to the hydrogen-bonded OH stretch of ADD water.[48,49] Because these ADD and AAD waters have nearly tetrahedral bonding geometries, the increase of such water sites indicates the primary process producing partially 3-D hydrogen-bonded cage structures. At $n = 21$, the intensity of the AD water band substantially decreases and the AAD water band becomes predominant in the free OH region. This means that the hydrogen bond network of $[C_6H_6-(H_2O)_n]^+$ consists only of three-coordinated waters from the $n = 21$ cluster, and formation of a closed 3-D cage structure is completed, as schematically shown in Figure 2c.

The hydrogen bond network evolution from the chain forms ($n \lesssim 10$) to the net forms ($10 \approx n \approx 20$) and then to the cage forms ($n \geq 21$) in the benzene−water cluster cations is remarkably similar to that observed in the protonated water clusters.[29,30] No pronounced effect of the phenyl radical can be found for the hydrogen bond network development. It should be, however, noted that the size correspondence between the IR spectra of the benzene−water cluster cations and protonated water clusters is different in the small-sized and large-sized clusters. For the small-sized clusters of $n < 8$, as seen in Figure 3, the IR spectrum of $[C_6H_6-(H_2O)_n]^+$ is clearly similar to that of $H^+(H_2O)_{n+1}$ (i.e., $H_2O-H^+(H_2O)_n$). This means that the phenyl radical plays the same role as one water molecule in the hydrogen bond network at this size range, and it may directly coordinate to the H_3O^+ (or $H_5O_2^+$) ion core with a σ-type hydrogen bond. This is because the protonated ion core is produced by the proton transfer from the C−H bond of the benzene cation moiety. A schematic picture for this size range was already given in Figure 2a. On the other hand, the water

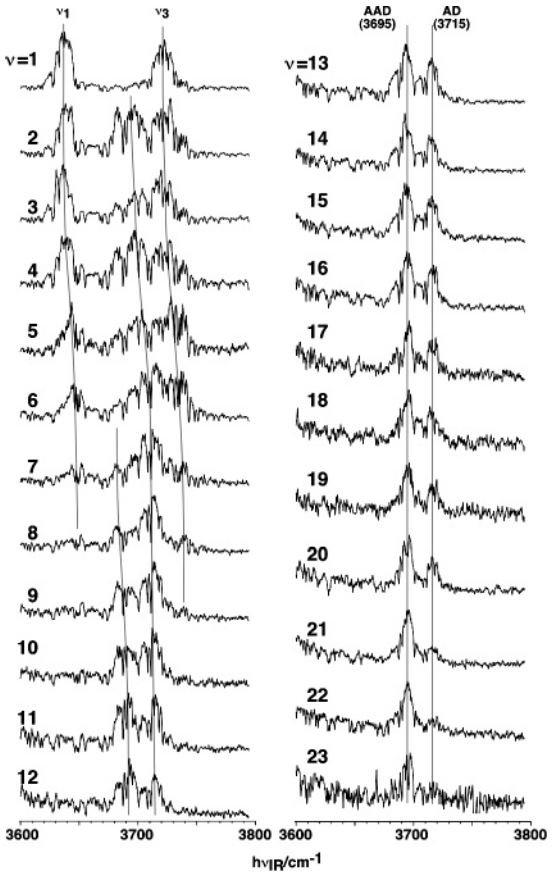

Figure 4. An expanded view of the free OH stretch region of the IR spectra of $[C_6H_6-(H_2O)_n]^+$ ($n = 1-23$). Bands appearing at 3650 and 3750 cm^{-1} are assigned to the symmetric (ν_1) and antisymmetric (ν_3) OH stretch vibrations, respectively, of a terminal water molecule in a hydrogen bond chain. Bands at 3695 cm^{-1} are the dangling OH stretch of three-coordinated (AAD) water. Bands at 3715 cm^{-1} are due to the dangling OH stretch of two-coordinated (AD) water. Sharp dips seen in the spectra are due to the IR absorption by the atmospheric water in the optical path.

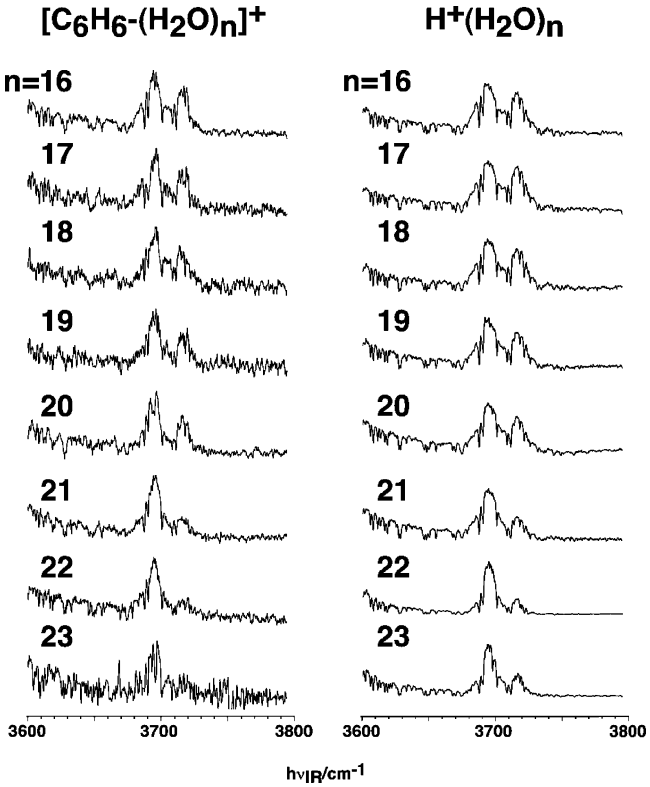

Figure 5. Comparison of the free OH region of the IR spectra of $[C_6H_6-(H_2O)_n]^+$ and $H^+(H_2O)_n$ in the large cluster sizes. Note that the definition of the cluster size, n, of the protonated water clusters is different from that in Figure 3.

cage formation is completed at the same size ($n = 21$) in both the benzene−water cluster cations and protonated water clusters. This is clearly demonstrated in the comparison of the free OH stretch region of the IR spectra of $[C_6H_6-(H_2O)_n]^+$ and $H^+(H_2O)_n$, as seen in Figure 5 (note that the size definition of the protonated water cluster is different from that in Figure 3). In this size region, the water molecules form the exclusive hydrogen bond network and the phenyl radical is pushed out from the network. Such a change of the size correspondence of the spectra implies that the role of the phenyl radical in the solvation structure is switched between $n = 8$ and $n = 20$. Because of the very gradual change of the spectral feature in this region, it is difficult to identify a unique onset of the switching only on the basis of the IR spectra. When we consider the nature of the hydrogen bond, however, it is quite reasonable to suppose that this switching of the solvation structures occurs with the evolution of the network structure from the chain to the net type. In the net-type structure, each water molecule contributes to at least two hydrogen bonds. The collaboration effect among hydrogen bonds enhances the hydrogen bond strength so that the binding energy of water molecules is larger than the simple sum of the binding energies of isolated hydrogen bonds, which is estimated to be about 1500 cm^{-1} in neutral water dimer.[51,52] With respect to this point, phenyl radical has a disadvantage to join the complicated network because phenyl radical can only be a single-proton acceptor in hydrogen bond formation, and its presence disturbs the evolution of the 2-D and 3-D network structures, which are more stable forms for large-sized clusters. Therefore, the phenyl radical is finally pushed out from the hydrogen bond network at $n \approx 10$, and a change of the size correspondence of the IR spectra occurs. The formation of the exclusive water moiety can be regarded as the primary process of the microscopic hydrophobicity. Of course, we note that the cage structure of water would be specific in the gas phase, and we should be careful to generalize the present result to the hydrophobicity in solutions.

The nuclear distance between the diagonal hydrogen atoms in phenyl radical is ∼0.5 nm, while the cavity size of the water cage (the nuclear distance between the diagonal oxygen atoms) at $n = 21$ is roughly estimated to be only 0.7−0.8 nm. In this respect, the phenyl radical cannot be accommodated in the cage of the observed cluster sizes, and it should be attracted to the surface of the water cage. Because it has been reported that phenyl radical prefers a π-type interaction rather than a σ-type interaction to form a cluster with a metal cation of a closed-shell electronic structure,[53] we suppose a π-hydrogen-bonded structure, where one of the dangling OH bonds of the water moiety is bound to the π-electrons of the phenyl radical (like in neutral $C_6H_6-(H_2O)_n$),[48] for the large-sized cluster cations. At the present stage, however, we have no experimental data to distinguish the σ- and π-type interactions between the phenyl radical and water moiety in the large-sized clusters, and this π-type hydrogen-bonded structure is still tentative. We observed a metastable decay of the parent cluster cation with an efficiency of a few percent in the second mass filter. Thus, the internal energy of the clusters in the present experiment is rather high, so that it is reasonable to expect that the bonding site with the phenyl radical may migrate on the surface of the water cage.

In the present measurement, any fragment species due to the evaporation of the phenyl radical were not found with the IR

irradiation, despite the evaporation of a few water molecules taking place in the large-sized clusters of $n \lesssim 15$. This preference for the water evaporation over phenyl radical might be a result from the extensive intracluster vibrational energy redistribution prior to the dissociation though the dissociation dynamics of the cluster cations has not yet been well studied at present.

Conclusion

In this study we carried out IR dissociation spectroscopy of the size-selected $[C_6H_6-(H_2O)_n]^+$ ($n = 1-23$) clusters prepared by collisions between photoionized benzene and water. The IR spectra in the OH and CH stretch regions showed that the cluster is regarded as a hydrated benzene cation at $n \leq 3$ while phenyl radical and protonated water are formed by the intracluster proton-transfer reaction at $n \geq 4$. The spectral features of the water moiety were almost identical with those of the protonated water clusters, despite the presence of phenyl radical in the clusters. This result clearly demonstrates that the hydrogen bond network evolution of the water moiety is essentially the same as that in $H^+(H_2O)_n$, where chain-type structures extending from the H_3O^+ (or $H_5O_2^+$) ion core develop into 2-D net-type structures at $n \approx 10$ and then the 3-D cage formation is completed at $n = 21$. The phenyl radical plays the same role as a water molecule in the solvation of the ion core in the small-sized clusters ($n \lesssim 10$), but it is pushed out from the exclusive hydrogen bond network of the water molecules in the large-sized clusters. This phenomenon can be regarded as the primary process of the microscopic hydrophobicity.

References and Notes

(1) Marcus, Y. *Ion solvation*; Wiley: New York, 1985.
(2) Wayne, R. P. *Chemistry of Atomospheres*; Oxford University Press: Oxford, U.K., 1991.
(3) Jeffrey, G. A. *Hydrogen Bonding in Biological Structures*; Springer-Verlag: Berlin, 1991.
(4) N.-Schatteburg, G.; Bondybey, V. E. *Chem. Rev.* **2000**, *100*, 4059.
(5) Kebarle, P.; Searles, S. K.; Zolla, A.; Scarborough, J.; Arshadi, M. *J. Am. Chem. Soc.* **1967**, *89*, 6393.
(6) Cunningham, A. J.; Payzant, J. D.; Kebarle, P. *J. Am. Chem. Soc.* **1972**, *94*, 7627.
(7) Meot-Ner, M.; Speller, C. V. *J. Phys. Chem.* **1986**, *90*, 6616.
(8) Magnera, T. F.; David, E. D.; Michl, J. *Chem. Phys. Lett.* **1991**, *182*, 363.
(9) Shi, Z.; Ford, J. V.; Wei, S.; Castleman, A. W. Jr. *J. Chem. Phys.* **1993**, *99*, 8009.
(10) Dalleska, N. F.; Honma, K.; Armentrout, P. B. *J. Am. Chem. Soc.* **1993**, *115*, 12125.
(11) Newton, M. D.; Ehrenson, S. *J. Am. Chem. Soc.* **1971**, *93*, 4971.
(12) Newton, M. D. *J. Chem. Phys.* **1977**, *67*, 5535.
(13) Del Bene, J. E.; Frisch, M. J.; Pople, J. A. *J. Phys. Chem.* **1985**, *89*, 3669.
(14) Frisch, M. J.; Del Bene, J. E.; Binkley, J. S.; Schaefer, H. F., III. *J. Chem. Phys.* **1986**, *84*, 2279.
(15) Xie, Y.; Remington, R. B.; Schaefer, H. F., III. *J. Chem. Phys.* **1994**, *101*, 4878.
(16) Svanberg, M.; Pettersson, J. B. C. *J. Phys. Chem. A* **1998**, *102*, 1865.
(17) Wei, D.; Salahub, D. R. *J. Chem. Phys.* **1997**, *106*, 6086.
(18) Singer, S. J.; McDonald, S.; Ojamäe, L. *J. Chem. Phys.* **2000**, *112*, 710.
(19) Khan, A. *Chem. Phys. Lett.* **2000**, *319*, 440.
(20) Hodges, M. P.; Wales, D. J. *Chem. Phys. Lett.* **2000**, *324*, 279.
(21) Mejías, J. A.; Lago, S. *J. Chem. Phys.* **2000**, *113*, 7306.
(22) Yeh, L. I.; Okumura, M.; Myers, J. D.; Lee, Y. T. *J. Chem. Phys.* **1989**, *91*, 7319.
(23) Okumura, M.; Yeh, L. I.; Myers, J. D.; Lee, Y. T. *J. Phys. Chem.* **1990**, *94*, 3416.
(24) Jiang, J.-C.; Wang, Y.-S.; Chang, H.-C.; Lin, S. H.; Lee, Y. T.; N.-Schatteburg, G.; Chang, H.-C. *J. Am. Chem. Soc.* **2000**, *122*, 1398.
(25) Chaudhuri, C.; Wang, Y.-S.; Jiang, J. C.; Lee, Y. T.; Chang, H.-C.; N.-Schatteburg, G. *Mol. Phys.* **2001**, *99*, 1161.
(26) Nagashima, U.; Nishi, N.; Tanaka, H. *J. Chem. Phys.* **1986**, *84*, 209.
(27) Lee, S.-W.; Freivogel, P.; Schindler, T.; Beauchamp, J. L. *J. Am. Chem. Soc.* **1998**, *120*, 11758.
(28) Wei, S.; Shi, Z.; Castleman, A. W., Jr. *J. Chem. Phys.* **1991**, *94*, 3268.
(29) Miyazaki, M.; Fujii, A.; Ebata, T.; Mikami, N. *Science* **2004**, *304*, 1134.
(30) Shin, J.-W.; Hammer, N. I.; Diken, E. G.; Johnson, M. A.; Walters, R. S.; Jaeger, T. D.; Duncan, M. A.; Christie, R. A.; Jordan, K. D. *Science* **2004**, *304*, 1137.
(31) Wu, C.-C.; Jiang, J. C.; Boo, D. W.; Lin, S. H.; Lee, Y. T.; Chang, H.-C. *J. Chem. Phys.* **2000**, *112*, 176.
(32) Chang, H.-C.; Jiang, J.-C.; Hahndorf, I.; Lin, S. H.; Lee, Y. T.; Chang, H.-C. *J. Am. Chem. Soc.* **1999**, *121*, 4443.
(33) Sawamura, T.; Fujii, A.; Sato, S.; Ebata, T.; Mikami, N. *J. Phys. Chem.* **1996**, *100*, 8131.
(34) Kleinermanns, K.; Janzen, Ch.; Spangenberg, D.; Gerhards, M. *J. Phys. Chem. A* **1999**, *103*, 5232.
(35) Shi, Z.; Wei, S.; Ford, J. V.; Castleman, A. W., Jr. *Chem. Phys. Lett.* **1992**, *200*, 142.
(36) Selinger, A.; Castleman A. W., Jr. *J. Phys. Chem.* **1991**, *95*, 8442.
(37) Steel, E. A.; Merz, K. M., Jr.; Selinger, A.; Castleman, A. W., Jr. *J. Phys. Chem.* **1995**, *99*, 7829.
(38) Sobott, F.; Wattenberg, A.; Barth, H.-D.; Brutschy, B. *Int. J. Mass Spectrom.* **1999**, *185*, 271.
(39) Hartke, B.; Charvat, A.; Reich, M.; Abel, B. *J. Chem. Phys.* **2002**, *116*, 3588.
(40) Khan, A. *Chem. Phys. Lett.* **2004**, *388*, 342.
(41) Miyazaki, M.; Fujii, A.; Ebata, T.; Mikami, N. *Phys. Chem. Chem. Phys.* **2003**, *5*, 1137.
(42) Miyazaki, M.; Fujii, A.; Ebata, T.; Mikami, N. *Chem. Phys. Lett.*, in press.
(43) Solcà, N.; Dopfer, O. *J. Phys. Chem. A* **2003**, *107*, 4046.
(44) Courty, A.; Mons, M.; Calvé, J. L.; Piuzzi, F.; Dimicoli, I. *J. Phys. Chem. A* **1997**, *101*, 1445.
(45) Buch, V.; Devlin, J. P. *J. Chem. Phys.* **1991**, *94*, 4091.
(46) Jiang, J. C.; Chang, J.-C.; Wang, B.-C.; Lin, S. H.; Lee, Y. T.; Chang, H.-C. *Chem. Phys. Lett.* **1998**, *289*, 373.
(47) Rowland, B.; Fisher, M.; Devlin, J. P. *J. Chem. Phys.* **1991**, *95*, 1378.
(48) Gruenloh, C. J.; Carney, J. R.; Arrington, C. A.; Zwier, T. S.; Fredericks, S. Y.; Jordan, K. D. *Science* **1997**, *276*, 1678.
(49) Buck, U.; Ettischer, I.; Melzer, M.; Buch, V.; Sadlej, J. *Phys. Rev. Lett.* **1998**, *80*, 2578.
(50) Devlin, J. P.; Sadlej, J.; Buch, V. *J. Phys. Chem. A* **2001**, *105*, 974.
(51) Klopper, W.; Rijdt, J. G. C. M. v. D.-v. d.; Duijneveldt, F. B. v. *Phys. Chem. Chem. Phys.* **2000**, *2*, 2227.
(52) Goldman, N.; Fellers, R. S.; Brown, M. G.; Braly, L. B.; Keoshian, C. J.; Leforestier, C.; Saykally, R. J. *J. Chem. Phys.* **2002**, *116*, 10148.
(53) Petrie, S. *Int. J. Mass Spectrom.* **2003**, *227*, 33.